

## Article

# Metabolomic Prediction of Cadmium Nephrotoxicity in the Snail *Helix aspersa maxima*

Aude Devalckeneer <sup>1</sup>, Marion Bouvriez <sup>1</sup>, Amandine Gautier <sup>2</sup> and Jean-Marie Colet <sup>1,\*</sup>

<sup>1</sup> Laboratory of Human Biology & Toxicology, Faculty of Medicine and Pharmacy, University of Mons, 7000 Mons, Belgium; aude.devalckeneer@umons.ac.be (A.D.)

<sup>2</sup> HEPH (Haute Ecole Provinciale du Hainaut), Condorcet, 7000 Mons, Belgium

\* Correspondence: jean-marie.colet@umons.ac.be

**Abstract:** The decontamination of polluted soils is a major socioeconomic issue in many industrialized countries. In situ remediation approaches are nowadays preferred to ex situ techniques, but they require among others the use of bioindicators, which are sensitive to the progressive depollution on health effects. Animal species have been mainly used so far to monitor aquatic and air pollution. Current research focuses on the development of living indicators of soil pollution. In this study, the garden snail *Helix aspersa maxima* was acutely exposed to cadmium, one major soil contaminant causing severe health effects, including nephrotoxicity. Kidney and hemolymph were sampled and analyzed by a <sup>1</sup>H-NMR-based metabolomic approach. Shortly after Cd exposure, numerous metabolic changes occurred in the hemolymph and kidney extracts. Altogether, they were indicative of a switch in energy sources from the Krebs cycle towards b-oxidation and the utilization of stored galactogen polysaccharides. Then, the activation of antioxidant defenses in the renal cells was suggested by the alteration in some precursors of glutathione synthesis, such as glutamate, and by the release of the antioxidant anserin. Cell membrane damage was evidenced by the increased levels of some osmolytes, betaine and putrescine, as well as by a membrane repair mechanism involving choline. Finally, the development of metabolic acidosis was suggested by the elevation in 3-HMG in the hemolymph, and the more pronounced lysine levels were consistent with acute excretion troubles. Cd-induced renal damage was objectified by the increased level of riboflavin, a recognized biomarker of nephrotoxicity.

**Keywords:** cadmium; nephrotoxicity; invertebrates; <sup>1</sup>H-NMR metabolomics



**Citation:** Devalckeneer, A.; Bouvriez, M.; Gautier, A.; Colet, J.-M. Metabolomic Prediction of Cadmium Nephrotoxicity in the Snail *Helix aspersa maxima*. *Metabolites* **2024**, *14*, 455. <https://doi.org/10.3390/metabo14080455>

Academic Editor: Christian Bock

Received: 4 July 2024

Revised: 2 August 2024

Accepted: 13 August 2024

Published: 17 August 2024



**Copyright:** © 2024 by the authors. Licensee MDPI, Basel, Switzerland. This article is an open access article distributed under the terms and conditions of the Creative Commons Attribution (CC BY) license (<https://creativecommons.org/licenses/by/4.0/>).

## 1. Introduction

Past exploitation of soil by coking plants and other petrochemical activity sites has given way today to industrial wastelands that are generally extremely polluted, notably by inorganic elements, including heavy metals such as cadmium. Until recently, the remediation of such polluted soils involved their excavation and remote treatment. In addition to being very expensive, this ex situ approach involves a geographic and temporal movement of pollutants, increasing the risks for the operators and environment due to the possible dispersion of pollutants. In situ remediation approaches were more recently introduced to get rid of the technical, economic and environmental disadvantages mentioned above. Numerous in situ techniques are available, ranging from physical (ventilation, pumping, trapping, etc.) to chemical (washing, oxidation/reduction) to thermal to, last but not least, biological methods (biodegradation, bioventing, biosparging, phytoremediation).

In this context of soil depollution, the physicochemical analysis of soil provides information on the presence and concentrations of anthropogenic pollutants. However, this analysis does not provide any clues on the effects of these contaminants on living systems. Therefore, it is essential to use bioindicators to complement these data when assessing pollution [1–3]. These bioindicators can be plant, fungal or animal species present in the contaminated environment (passive use) or established as part of the study (active use). Two

types of bioindicators are currently described, namely accumulation indicators and effect or impact indicators. The use of animal bioindicator species has until now been mainly applied to monitoring aquatic pollution (plankton, mussels, “MODIOLE”, “RINBIO” programs) [4–6] and air pollution (insects, etc.) [7]. Current research focuses on the development of biological indicators (earthworms, microorganisms, snails) [8] to specifically assess the risk of soil pollution. *Helix aspersa maxima* (Taylor, 1883) [9] is a garden snail of a 20–30 g body weight (b.w.). It originates from North Africa and is considered as a promising alternative model. Terrestrial gastropods are well known for bioaccumulating and neutralizing trace metals either in lysosomal granules and by excretion or by methallothionein binding [10]. The digestive gland of snails has a high affinity for metals due to its ability to absorb particulate materials. The surrounding cells of the digestive gland, including renal cells, are responsible for the absorption, phagocytosis, accumulation and excretion of metals during digestion [11]. Thereby, the kidney is associated to the absorption and urine excretion of these compounds [12].

The biological responses of those bioindicator organisms to toxic exposure result in a change at the biochemical, physiological or behavioral levels. These changes, called toxicity biomarkers [13], can be observable (chlorosis, necrosis, weight loss, loss of pigmentation) and/or measurable (biomass, growth, protein dosage and enzymatic activity) [14,15]. One drawback of this multifactorial approach is the large number of assays that must be carried out to evaluate each individual biomarker. One promising alternative is nowadays proposed by the omics methods, which allows for a more global assessment of the changes in one single analysis. In particular, metabolomics offers a global survey of the alterations in the metabolome, namely, all small organic molecules, players in biochemical and cellular signaling pathways. In this study, we evaluated the potential of combining an invertebrate organism bioindicator of soil pollution with a metabolomics analytical approach to assess Cd-induced nephrotoxicity. To determine this, snails (*Helix aspersa maxima*) were exposed to cadmium (Cd) and we analyzed kidney extracts and hemolymph samples using a <sup>1</sup>H-NMR-based metabolomic approach.

## 2. Materials and Methods

### 2.1. Animal Housing

All animal experiments were carried out on an invertebrate species, the snail *Helix aspersa maxima*, for which there is no official regulation of animal welfare in Belgium.

*Helix aspersa maxima* individuals were purchased from the helicicole farm of Avesnois (Croix-Caluyau, France) and housed in plastic boxes with permanent access to water and professional food farming provided by the Helinove product (Saint-Paul-en-Pareds, France). They were kept at a temperature of 20 ± 2 °C and daylighting. Only adults with a matching age and body weight (~20 g) were investigated. A total of 24 snails were used in this study, with 6 individuals per group.

### 2.2. Chemicals

Phosphate buffer–D<sub>2</sub>O was prepared with Na<sub>2</sub>HPO<sub>4</sub>·2H<sub>2</sub>O 0.2 M and NaH<sub>2</sub>PO<sub>4</sub>·H<sub>2</sub>O 0.04 M in distilled water–deuterium oxide (D<sub>2</sub>O) solution (80:20, v:v); methanol; chloroform; TSP (deuterated sodium 3-trimethylsilyl propionate); and CdCl<sub>2</sub> (cadmium chloride 99.9%, from Alfa Aesar Chemicals, Thermo Fisher Scientific, Waltham, MA, USA).

### 2.3. Cd Exposure

First, the dose of cadmium to which the snails were exposed was selected from the literature data on rodent models [16]. *Helix aspersa maxima* snails (*n* = 12) received an intramuscular injection of 4 mg/kg of Cd. Injections were applied in the posterior part of the foot to minimize the risk of damaging any vital organ of the body with the needle while allowing a systemic distribution of Cd after its absorption in the hemolymph. After either 4 h (*n* = 6) or 24 h (*n* = 6) of exposure, the hemolymph was sampled before killing the individuals by freezing them at –20 °C. Control individuals (*n* = 12) were exposed

according to the same protocol to distilled water, solvent used for the preparation of Cd solution. Snails were dissected on ice to sample the digestive gland and kidney tissues, which were immediately frozen in liquid nitrogen and stored at  $-80\text{ }^{\circ}\text{C}$  until further measurements of enzymatic activity and  $^1\text{H-NMR}$  spectroscopy.

#### 2.4. Hemolymph Sampling

The procedure used in this study was based on the validated protocol previously described by Cooper et al. (1993) [17]. Briefly, snails were washed in cold water to remove feces and excess mucus before hemolymph sampling. Snails were placed upside down and a 25 G needle was inserted just below the pneumostome to allow hemolymph to flow out. An amount of 500  $\mu\text{L}$  of a pale blue colored liquid was collected in Eppendorf tubes. Amicon<sup>®</sup> Ultra-0.5 Centrifugal Filter Devices (Millipore, Merck Group, Darmstadt, Germany) were rinsed four times with 500  $\mu\text{L}$  of demineralized water and centrifuged for 15 min at  $14,000\times g$ . Then, 500  $\mu\text{L}$  of hemolymph was filtered and centrifuged (30 min at  $14,000\times g$ ) before adding 250  $\mu\text{L}$  of  $\text{D}_2\text{O}$  and centrifuging again (30 min at  $14,000\times g$ ). Filtrates were kept at  $-80\text{ }^{\circ}\text{C}$  until  $^1\text{H-NMR}$  analysis.

#### 2.5. $^1\text{H-NMR}$ Spectroscopy and Spectral Data Analysis

The procedure of sample preparation and  $^1\text{H-NMR}$  spectroscopy on tissue extracts used in this study was based on an in-house method developed on *Helix aspersa maxima* tissues [18], derived from the validated protocol previously described by Beckonert et al. (2007) [19].

##### 2.5.1. Sample Preparation

Kidney tissue samples preserved at  $-80\text{ }^{\circ}\text{C}$  were crushed in a mortar with liquid nitrogen into powder and were extracted with precooled solutions according to a methanol–water–chloroform extraction method (volumes used per gram of organ): homogenization of the formed powder with 4 mL of methanol and 850  $\mu\text{L}$  of water with vortex, followed by 2 mL of chloroform with vortex before extra-homogenization with 2 mL of chloroform and 2 mL of water with vortex. The homogenates were placed on ice during 10 min before centrifugation (15 min at  $1000\times g$ ,  $4\text{ }^{\circ}\text{C}$ ). The top aqueous phase was retrieved, and methanol was removed in vacuo for 6 h. Each extract was reconstituted in 700  $\mu\text{L}$  phosphate buffer– $\text{D}_2\text{O}$  0.1 M before final centrifugation ( $10,000\times g$ , 10 min), and 50  $\mu\text{L}$  of TSP ( $\text{D}_4$ -trimethylsilyl propionic acid) 7 mM was added to 650  $\mu\text{L}$  supernatant. Regarding the hemolymph samples, 600  $\mu\text{L}$  of previously filtered preparations was mixed with 100  $\mu\text{L}$  of TSP 4 mM. TSP prepared in 100%  $\text{D}_2\text{O}$  was used as the external reference for the calibration of the NMR spectra. Its resonance was arbitrarily fixed at 0.00 ppm for further spectral calibration. Finally, 700  $\mu\text{L}$  of each sample were transferred into individual tubes (5 mm diameter) for NMR analysis.

##### 2.5.2. Acquisition of Metabolic Profiles

One-dimensional NMR spectra of extracts were acquired on a Bruker 500 Avance spectrometer (11.8 T corresponding to a proton Larmor frequency of 500 MHz) at 297 K using a NOESYPRESAT-1d pulse sequence. A total of 128 free induction decays (FIDs), with 65,536 data points per FID, were collected for tissue extraction using a spectral width of 10,330,578 Hz, an acquisition time of 3.17 s and a pulse recycle delay of 3 s. After Fourier transformation, all spectra were referenced to the chemical shift of the TSP (0.0 ppm) and were phase- and baseline-corrected using MestReNova 11.0 software (Mestrelab Research, Santiago de Compostela, Spain) and submitted to a line broadening of 0.3 Hz. After removing spectral regions distorted by imperfect water peak saturation, binning of the remaining areas reducing the spectral region from 0.08 to 10.00 ppm into 248 integrated regions (buckets) with a 0.04 ppm width each was applied. Each spectrum was normalized against the total sum of spectral integrals before multivariate analysis in SIMCA-P+ 12.0 software (Umetrics, Umea, Sweden). An unsupervised principal component analysis (PCA)

was used on pareto-scaled data to identify possible outlier samples and evaluate the degree of homogeneity before performing a supervised partial least square discriminant analysis (PLS-DA) to check on the possible clustering of samples by one-way cross-validation analysis of variance (CV-ANOVA) and possibly detect different metabolic patterns due to Cd exposure. The most efficient representation of the groups clustering given by the PLS-DA was the score plot and the corresponding loading plot was used to pick up discriminant metabolites. Metabolites were identified from their respective resonances, according to their chemical shift and multiplicity as compared to historical databases. The quality of the model was described by the  $R^2$  parameter, which represents the explained variation in the dataset, and the reliability was described by the  $Q^2$  parameter, which used cross-validation to estimate the goodness of prediction of the model.

### 2.5.3. Statistical Analysis

Discriminant metabolites were extracted with the variable important parameter (VIP) list of the PLS-DA model, which identified those with a cut-off VIP score  $\geq 1$  as mainly contributing to the clustering. For ease, the term “area under the curve” (AUC) is used in this work instead of “peak/bucket/feature areas”. A Mann–Whitney Wilcoxon statistical test was applied to the AUC values on those VIPs to assess the significance of metabolites responsible for intergroup differences ( $p$ -value  $< 0.05$  significance level) between Cd-exposed animals and their matching control fellows (4 h and 24 h). This non-parametric statistical test was chosen considering the semi-quantitative data provided by the AUC values.

## 3. Results

### 3.1. $^1\text{H-NMR}$ Profiles of Kidney Extracts Collected from Cd-Exposed Snails

The  $^1\text{H-NMR}$  spectra obtained from the kidney extracts of the Cd-exposed snails were submitted to multivariate data analyses and compared to the control individuals. The PLS-DA score scatter plot reported in Figure 1 revealed some clusters discriminating those snails exposed to 4 mg/Kg Cd for 4 h from their matched controls (Figure 1A,  $n = 6$ ), with good-quality values of  $R^2_x = 0.725$ ,  $R^2_y = 0.998$  and  $Q^2 = 0.76$ . The same observation was made between the animals exposed to Cd for 24 h and their respective timely controls with  $R^2_x = 0.488$ ,  $R^2_y = 0.963$  and  $Q^2 = 0.744$  (Figure 1C,  $n = 6$ ).

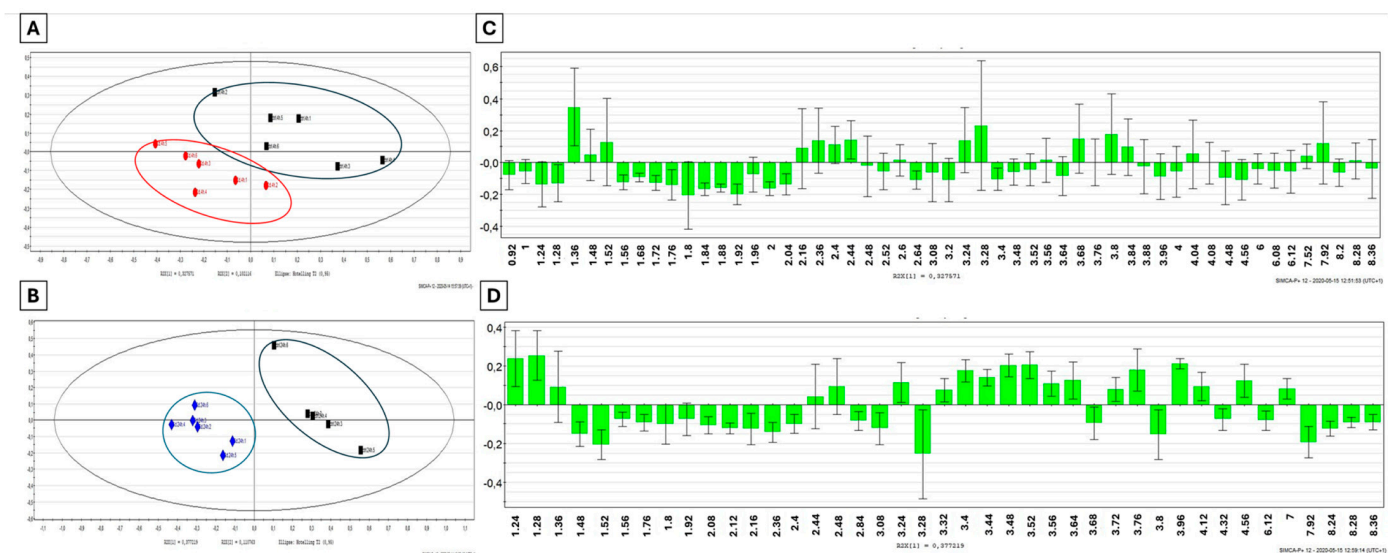


**Figure 1.** PLS-DA score scatter plots of  $^1\text{H-NMR}$  binned data obtained from kidney aqueous extracts from snails ( $n = 6$ ) exposed to 4 mg/Kg of Cd for (A) 4 h (in red) and (B) 24 h (in blue) compared to their timely control group (in black). Loading column plots of VIP chemical shifts extracted from the corresponding PLS-DA for Cd exposures (C) of 4 h and (D) 24 h, respectively.

The metabolites contributing to the clustering were identified according to their chemical shift and multiplicity of their corresponding resonances. Peak assignments in the kidney extracts of *Helix aspersa maxima* obtained by <sup>1</sup>H-NMR were previously described by Devalckeneer et al. (2019) [18] thanks to an in-house library based on the use of Chemonix NMR suite software (version 8.1.1) and the Human Metabolome Database (HMDB). Only those discriminant metabolites displaying a VIP score  $\geq 1$  were considered for further analysis and are presented in the loading column plots in Figure 1C,D for the 4 h and 24 h time points, respectively.

The changes in the levels of those discriminant metabolites in the renal tissue during Cd exposure are shown in the heatmap projection presented in Table 1: a redder tone indicates a higher renal concentration of the considered metabolite, while a greener tone indicates a lower concentration.

**Table 1.** Heatmap of discriminant metabolites in renal tissue with either increased levels (the higher levels in the redder tone) or decreased levels (the lower levels in the greener tone) in Cd-exposed groups as compared to their matching controls. Significant changes are displayed in italic bold character (Mann–Whitney Wilcoxon test,  $p$ -value < 0.05). Hydroxybut.: Hydroxybutyrate; N-acetyl-LY.: N-acetyl-Lysine;  $\beta$ -glc:  $\beta$ -glucose.

Metabolite	Isoleucine	Valine	Hydroxybut.	Fucose	Lactate					
Control	100	100	100	100	100					
4 h Cd	140	120	146	140	33					
24 h Cd	73	125	43	45	65					
Metabolite	Alanine	Putrescine	Acetate	N-acetyl-LY.	Glutamate					
Control	100	100	100	100	100					
4 h Cd	90	285	157	114	181					
24 h Cd	208	108	125	112	83					
Metabolite	Glutamine	Succinate	Riboflavine	Citrate	Aspartate					
Control	100	100	100	100	100					
4 h Cd	85	80	107	276	95					
24 h Cd	146	162	63	70	178					
Metabolite	Choline	Betaïne	Carnitine	$\beta$ -glc	Glycine					
Control	100	100	100	100	100					
4 h Cd	82	90	146	97	96					
24 h Cd	77	135	45	53	63					
Metabolite	Glycerol	Maltose	$\beta$ -Galactose	Adenosine	Anserine					
Control	100	100	100	100	100					
4 h Cd	120	115	201	147	152					
24 h Cd	73	66	44	214	47					
Metabolite	7.52 ppm	Urocanate	Hypoxanthine							
Control	100	100	100							
4 h Cd	71	80	164							
24 h Cd	52	225	181							
<i>High</i>	200	185	150	120	100	80	50	25	0	<i>Low</i>

Therefore, increased levels of valine, acetate, N-acetyl-lysine, adenosine and hypoxanthine were observed over time while the levels of lactate and choline decreased. Interestingly, some metabolites only changed after 24 h exposure, such as alanine, aspartate and betaine, which were increased, while riboflavin,  $\beta$ -glucose and glycine were decreased. Many metabolites also varied differently depending on the duration of exposure, namely isoleucine, hydroxybutyrate, fucose, glutamate, citrate, carnitine, glycerol, maltose,  $\beta$ -galactose and anserine, which increased after 4 h and decreased after 24 h compared to glutamine, succinate and urocanate, which followed the opposite evolution. All changes in metabolites following Cd exposure that turned out to be statistically significant according to the Mann–Whitney Wilcoxon test ( $p$ -value < 0.05) are indicated in bold in Table 1.

### 3.2. $^1\text{H-NMR}$ Profiles of Hemolymph Samples Collected from Cd-Exposed Snails

The hemolymph samples were analyzed by  $^1\text{H-NMR}$  spectroscopy and the obtained resonances were assigned to their corresponding metabolites based on their chemical shift and multiplicity by comparison with in-house data and databases freely accessible on the web (Figure 2).

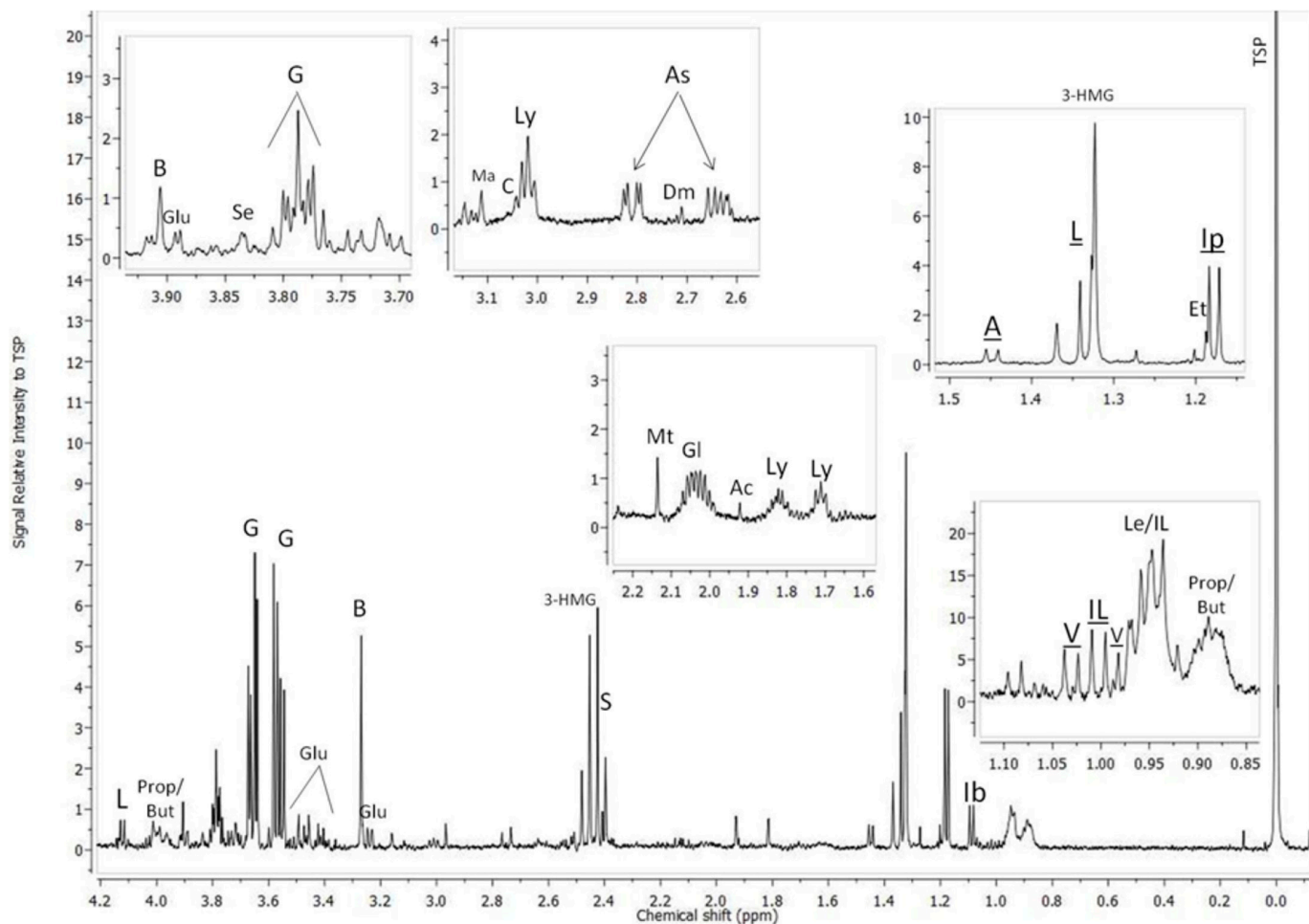


**Figure 2.** Identification of resonances from  $^1\text{H-NMR}$  spectra acquired at 500 MHz (128 scans) on hemolymph samples from *Helix aspersa maxima*. Peak assignments by comparison of their chemical shift and multiplicity with in-house and web databases (Chenomx NMR suite software, version 8.1.1). V: Valine, Le: Leucine, IL: Isoleucine, P&B: Propanoate/Butanoate regions, Ib: Isobutyrate, Ip: Isopropanol, Et: Ethanol, 3-HMG: 3-hydroxy-methylglutarate, L: Lactate, A: Alanine, Ly: Lysine, Ac: Acetate, Gl: Glutamate, Mt: Methionine, S: Succinate, As: Aspartate, Dm: Dimethylamine, C: Creatine, Ma: Malonate, Glu: Glucose, B: Betaine, G: Glycerol, Se: Serine.

The PLS-DA analysis allowed for the separation of the Cd-exposed group from its matching timely controls, as shown on the score scatter plot in Figure 3. Clusters observed after 4 h Cd exposure (Figure 3A,  $n = 6$ ) showed values of  $R^2_x = 0.873$ ,  $R^2_y = 0.996$  and  $Q^2 = 0.524$  and values of  $R^2_x = 0.92$ ,  $R^2_y = 0.999$  and  $Q^2 = 0.689$  after 24 h (Figure 3C,  $n = 6$ ), indicating good quality. VIP lists were extracted from each supervised multivariate analysis, pinpointing the discriminant descriptors (Figure 3C,D).

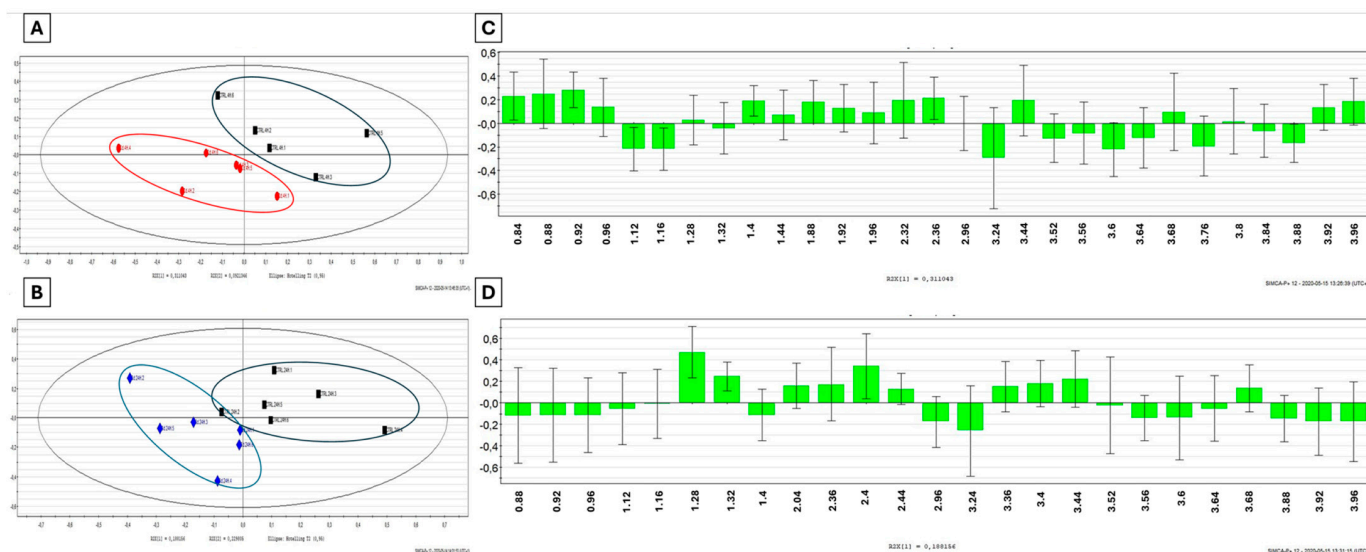


**Figure 3.** PLS-DA score scatter plots of  $^1\text{H-NMR}$  spectral data obtained from snail hemolymph ( $n = 6$ ) exposed to 4 mg/Kg of Cd for (A) 4 h (in red) and (B) 24 h (in blue) compared to their timely control group treated with distilled water (in black). Loading column plots of VIP chemical shifts extracted from corresponding PLS-DA for (C) 4 h and (D) 24 h Cd exposure.

The corresponding identified metabolites listed in Table 2 indicate a timely decrease in the levels of glutamate and glucose associated with increased levels of lysine and betaine. Changes observed after 4 h of exposure, such as increased levels of isobutyrate and isopropanol and decreased levels of acetate, were back to pre-exposure levels after 24 h. Isoleucine, alanine and the butanoate/propanoate region decreased after 4 h of Cd exposure but increased after 24 h. The opposite evolution was noticed for 3-hydroxy-methylglutarate (3-HMG). Changes in metabolites such as lactate, succinate and serine were only seen after 24 h Cd exposure, showing decreased concentrations.

**Table 2.** Heatmap of discriminant metabolites in hemolymph with either increased levels (the higher levels in the redder tone) or decreased levels (the lower levels in the greener tone) in Cd-exposed groups as compared to their matching controls. Isoprop.: Isopropanol; Prop/But: Propanoate/Butanoate regions; 3-HMG: 3-hydroxy-methylglutarate.

Metabolite	Isoleucine	Isobutyrate	Isoprop.	Lactate	Alanine
Control	100	100	100	100	100
4 h Cd	60	134	129	96	69
24 h Cd	149	106	101	42	121
Metabolite	Acetate	Glutamate	Succinate	Lysine	Glucose
Control	100	100	100	100	100
4 h Cd	60	81	100	122	79
24 h Cd	110	76	26	132	73
Metabolite	Glycerol	Serine	Prop/But	Betaine	3-HMG
Control	100	100	100	100	100
4 h Cd	106	97	73	127	155
24 h Cd	112	83	142	133	54
<b>High</b>	<b>200</b>	<b>185</b>	<b>150</b>	<b>120</b>	<b>100</b>
				<b>80</b>	<b>50</b>
					<b>25</b>
					<b>0</b>
					<b>Low</b>

#### 4. Discussion

##### *Metabolic Impact of Cd Exposure in Snails*

As most of the basic metabolic pathways are conserved among species through evolution, metabolic biomarkers present great interests in toxicology. Indeed, the enzymes from the glycolytic pathway and Krebs cycle have been identified for a long time in gastropod

tissues [20], as well as enzymes involved in the turnover of ketone bodies, which are also detectable in terrestrial mollusks [21].

Shortly after Cd exposure, an increase in the hydroxybutyrate level, a ketone body produced by fatty acid  $\beta$ -oxidation, was noticed in the kidney extracts, together with increased sugar sources such as maltose, fucose and galactose. The higher level of galactose, mainly stored as the polysaccharide galactogen in snails, could indicate a shift towards energy expenditure supported by both  $\beta$ -oxidation and ketogenesis, two major energy sources for renal cells. This increasing glycolytic flux combined with a slowing down of Krebs cycle activity, as witnessed by lower succinate production, were already observed in renal cell carcinoma by Monteiro et al. (2016) [22]. Likewise, an increase in the branched-chain amino acids valine and isoleucine were also observed in our study and by Zhong et al. (2012) [23] in the kidney extracts of rats with chronic kidney disease (CKD). However, the decrease in hydroxybutyrate and carnitine, two main actors of fatty acid metabolism, revealed a dysregulation of  $\beta$ -oxidation after 24 h of Cd exposure. Losses of glucose and other carbohydrates also indicated a lack of primary energy sources. The decreased levels of glutamate and serine in hemolymph confirmed the need for an energy supply, since both metabolites are involved in ATP synthesis. The early glutamate increases in kidney extracts from Cd-exposed snails was most likely correlated with the concomitant decreased levels of urocanate. As serine is a precursor of glycine, a component of glutathione (GSH) with glutamate, one could assume that its consumption supplies the cellular antioxidant defense within 24 h of Cd exposure.

Choline is a methyl donor involved in several physiological processes including the synthesis of phospholipids, essential structural components of cell membranes. The decreased level of choline observed as early as 4 h after the onset of Cd exposure is associated with deviant behavior in cell membrane metabolism. The same metabolic alteration was already reported in CKD patients and explained by a greater demand for phospholipids in replicating renal cells [24]. Choline may also be oxidized in liver and kidney mitochondria to betaine, an osmolyte protecting cell integrity against osmotic stress, especially in the kidney. Elevations in betaine and putrescine, other markers of osmotic stress, were observed in the kidney extracts and hemolymph from 4 h of exposure.

Anserine is a well-known and important buffer molecule in muscles, as well as an antioxidant and crucial promoter of glycolysis [25]. Riboflavin has been described as a biomarker of nephrotoxicity by Fuchs et al. (2011) [26], as well as a key player in muscle repair. Moreover, the metabolic acidosis episode described in CKD rats and leading to the catabolism of muscular proteins can also be appreciated from the higher levels of alanine together with a lowering in glutamate. Thus, the early (4 h) increased anserine level followed by the later (24 h) decreases in riboflavin and glutamate together with an increased alanine concentration could be indicative of the cellular response to Cd-induced renal damage followed by cellular repair, as already reported in rats developing renal failure.

Metabolic acidosis could as well be confirmed by the elevation in 3-HMG in the hemolymph, observed at 4 h exposure. 3-HMG is an intermediate in the leucine degradation process catalyzed by 3-HMG-CoA lyase, also playing a role in the production of ketone bodies. Metabolic acidosis, responsible for the oxidative stress and DNA injuries linked to 3-HMG, was also demonstrated by Deldago et al. (2019) [27].

Purine catabolism was also suspected in the snails during Cd exposure due to higher levels of hypoxanthine and adenosine. Both nitrogen bases can also be related to DNA injuries. Hypoxanthine is generally found in higher concentrations in the plasma of patients with kidney failures. Adenosine, though a nucleoside important in ATP formation, is also a signal molecule known to be induced in the cases of ischemia and hypoxia. Lysine is a major amino acid considered as a building block of most proteins, as well as a precursor of carnitine. Its early increase in the hemolymph of the Cd-exposed snails could be consistent with acute excretion troubles, as already noticed and reported in various types of acute renal failure in the rat [28].



Although this study focused on nephrotoxicity caused by cadmium, it is interesting to note that certain metabolic changes could also reflect nervous system toxicity, another known adverse effect of this heavy metal. Thus, as glutamate and serine are either directly or indirectly involved in neurotransmission, they could be indicative of neurotoxicity. Likewise, as a precursor of acetylcholine and considering the importance of a methyl donor like choline for brain function, decreasing choline could be used to compensate for neuronal injuries. Finally, the accumulation of 3-HMG in biological fluids is a metabolic disorder in patients characterized by a 3-HMG-CoA lyase deficiency and presenting neurological symptoms, especially during metabolic crises [29]. Da Rosa et al. (2013) [30] showed that 3-HMG induces protein oxidative damage in the brain and GSH deprivation leading to a reduction in antioxidant defenses.

## 5. Conclusions

In conclusion, this study demonstrated the potential of combining an “omics” tool with a bioindicator invertebrate model, herein the *Helix aspersa maxima* snail, in prospective risk assessment. This approach could help in monitoring the effectiveness of soil depollution in the future.

**Author Contributions:** Conceptualization, A.D.; methodology, A.D.; formal analysis, A.D.; investigation, A.D., M.B. and A.G.; resources, A.D. and J.-M.C.; data curation, A.D.; writing—original draft preparation, A.D.; writing—review and editing, J.-M.C.; supervision, J.-M.C.; funding acquisition, A.D. and J.-M.C. All authors have read and agreed to the published version of the manuscript.

**Funding:** This research was funded by GreenWin (Convention 7276), The Walloon Region, Belgium.

**Institutional Review Board Statement:** Ethical review and approval were waived for this study due to no official regulation of animal welfare in Belgium on invertebrates animals as snails.

**Informed Consent Statement:** Not applicable.

**Data Availability Statement:** The original contributions presented in the study are included in the article.

**Acknowledgments:** The authors acknowledge C. Henoumont from UMONS for her precious contribution to this work.

**Conflicts of Interest:** The authors declare no conflicts of interest.

## References

1. Ribera, D.; Taberly, J. *Mélanges de Polluants, Toxicité, Écotoxicité et Évaluation des Risques*. Etude RECORD n°08-0668/1A. 2011. 295p. Available online: <https://record-net.org/media/etudes/38/public/synthese/synth-record08-0668-1a.pdf> (accessed on 3 July 2024).
2. Lavelle, P.; Spain, A.V. *Soil Ecology*; Kluwer Scientific: Amsterdam, The Netherlands, 2001.
3. Lavelle, P.; Decaëns, T.; Aubert, M.; Barrot, S.; Blouin, M.; Bureau, F.; Margerie, P.; Mora, P.; Rossi, J.-P. Soil invertebrates and ecosystem services. *Eur. J. Soil Biol.* **2006**, *42*, S3–S15. [CrossRef]
4. Andral, B.; Galgani, F.; Tomasino, C.; Bouchoucha, M.; Blottiere, C.; Scarpato, A.; Benedicto, J.; Deudero, S.; Calvo, M.; Alexandro, C.; et al. Chemical contamination baseline in the Western basin of the Mediterranean Sea based on transplanted mussels. *Arch. Environ. Contam. Toxicol.* **2011**, *61*, 261–271. [CrossRef] [PubMed]
5. Tanabe, S.; Prudente, M.S.; Kanatireklap, S.; Subramanian, A. Mussel watch: Marine pollution monitoring of butyltins and organochlorines in coastal waters of Thailand, Philippines and India. *Ocean. Coast. Manag.* **2000**, *43*, 819–839. [CrossRef]
6. Regoli, F.; Orlando, E. *Mytilus galloprovincialis* as a bioindicator of lead pollution: Biological variables and cellular responses. *Sci. Total Environ.* **1993**, *134*, 1283–1292. [CrossRef]
7. Conti, M.E.; Botré, F. Honeybees and Their Products as Potential Bio-Indicators of Heavy Metal Contamination. *Environ. Monit. Assess.* **2001**, *69*, 267–282. [CrossRef]
8. Pérès, G.; Vandenbulcke, F.; Guernion, M.; Hedde, M.; Beguiristain, T.; Douay, F.; Houot, S.; Piron, D.; Richard, A.; Bispo, A.; et al. Earthworm indicators as tools for soil monitoring, characterization and risk assessment: An example from the national Bioindicator programme. *Pedobiol. Int. J. Soil Biol.* **2011**, *54*, S77–S87. [CrossRef]
9. Taylor, J.W. Life history of British Helices: *Helix (Pomatia) aspersa* Müll. *J. Conchol.* **1883**, *4*, 94.
10. Grara, N.; Boucenna, M.; Atailia, A.; Berrebbah, H.; Djebar, M.R. Stress oxydatif des poussières métalliques du complexe sidérurgique d’Annaba (Nord-Est algérien) chez l’escargot *Helix aspersa*. *Environ. Risques Santé* **2012**, *11*, 221–229.

11. Chabircovsky, M.; Niederstätter, H.; Thaler, R.; Hödl, E.; Parson, W.; Ross Manith, V.; Dallinger, R. Localization and quantification of Cd- and Cu-specific metallothionein isoform mRNA in cells and organs of the terrestrial gastropod *Helix pomatia*. *Toxicol. Appl. Pharm.* **2003**, *190*, 25–36. [[CrossRef](#)] [[PubMed](#)]
12. Coeurdassier, M. Utilisation de Mollusques Gastéropodes Pulmonés Terrestres (*Helix aspersa*) et Aquatiques (*Lymnia stagnalis* et *Lymnia palustris*) Comme Indicateurs de Pollution par les Éléments Métalliques et les Xénobiotiques. Ph.D. Thesis, Université de Franche-Comté, Besançon, France, 2001; 281p.
13. Lagadic, L.; Caquet, T.; Amiard, J.-C. Biomarqueurs en écotoxicologie: Principes et définitions. In *Biomarqueurs en Ecotoxicologie: Aspects Fondamentaux*; Lagadic, L., Caquet, T., Amiard, J.-C., Ramade, F., Eds.; Collection d'Ecologie; Masson Editeur: Paris, France, 1997; pp. 1–9.
14. Bocquené, G.; Galgani, F.; Truquet, P. Characterization and assay conditions for use of AChE activity from several marine species in pollution monitoring. *Mar. Environ. Res.* **1990**, *30*, 75–89. [[CrossRef](#)]
15. Bucheli, T.D.; Fent, K. Induction of Cytochrome P450 as a Biomarker for Environmental Contamination in Aquatic Ecosystems. *Crit. Rev. Environ. Sci. Technol.* **1995**, *25*, 201–268. [[CrossRef](#)]
16. Fasitsas, D.; Theocharis, S.E.; Zoulas, D.; Chrissimou, S.; Deliconstantinos, G. Time-dependent cadmium-neurotoxicity in rat brain synaptosomal plasma membranes. *Comp. Biochem. Physiol. Part C Comp. Pharmacol.* **1991**, *100*, 271–275. [[CrossRef](#)] [[PubMed](#)]
17. Cooper, J.E. Bleeding of pulmonate snails. *Lab. Anim.* **1994**, *28*, 277–278. [[CrossRef](#)]
18. Devalckeneer, A.; Marion, B.; Raphaël, C.; Colet, J.-M. Proton Nuclear Magnetic Resonance (<sup>1</sup>H NMR) profiling of isolated organs in the snail *Helix aspersa maxima*. *Ecol. Indic.* **2019**, *105*, 177–187.
19. Beckonert, O.; Keun, H.C.; Ebbels, T.M.D.; Bundy, J.; Holmes, E.; Lindon, J.C. Metabolic profiling, metabolomic and metabonomic procedures for NMR spectroscopy of urine, plasma, serum and tissue extracts. *Nat. Protoc.* **2007**, *2*, 2692–2703. [[CrossRef](#)] [[PubMed](#)]
20. Hochachka, P.W.; Fields, J.H.A.; Mommsen, T.P. Metabolic and enzyme regulation during rest-to-work transition: A mammal versus mollusc comparison. In *The Mollusca, Volume 1. Metabolic Biochemistry and Molecular Biomechanics*; Hochachka, P.W., Ed.; Elsevier: Amsterdam, The Netherlands, 1983; pp. 55–89.
21. Stuart, J.A.; Ballantyne, J.S. Subcellular organization of intermediary metabolism in the hepatopancreas of the terrestrial snail, *Cepaea nemoralis*: A cytosolic  $\beta$ -hydroxybutyrate dehydrogenase. *J. Exp. Zool.* **1996**, *274*, 291–299. [[CrossRef](#)]
22. Monteiro, M.S.; Barros, A.S.; Pinto, J.; Carvalho, M.; Pires-Luís, A.S.; Henrique, R.; Jerónimo, C.; Bastos, M.d.L.; Gil, A.M.; de Pinho, P.G. Nuclear Magnetic Resonance metabolomics reveals an excretory metabolic signature of renal cell carcinoma. *Sci. Rep.* **2016**, *6*, 37275. [[CrossRef](#)] [[PubMed](#)]
23. Zhong, F.; Liu, X.; Zhou, Q.; Hao, X.; Lu, Y.; Guo, S.; Wang, W.; Lin, D.; Chen, N. <sup>1</sup>H NMR spectroscopy analysis of metabolites in the kidneys provides new insight into pathophysiological mechanisms: Applications for treatment with *Cordyceps sinensis*. *Nephrol. Dial. Transplant.* **2012**, *27*, 556–565. [[CrossRef](#)]
24. Qi, S.; Ouyang, X.; Wang, L.; Peng, W.; Wen, J.; Dai, Y. A Pilot Metabolic Profiling Study in Serum of Patients with Chronic Kidney Disease Based on <sup>1</sup>H-NMR-Spectroscopy. *Clin. Transl. Sci.* **2012**, *5*, 379–385. [[CrossRef](#)] [[PubMed](#)]
25. Le Roy, C.I.; Mappley, L.J.; La Ragione, R.M.; Woodward, M.J.; Claus, S.P. NMR-based metabolic characterization of chicken tissues and biofluids: A model for avian research. *Metabolomics* **2016**, *12*, 157. [[CrossRef](#)] [[PubMed](#)]
26. Fuchs, T.C.; Hewitt, P. Biomarkers for Drug-Induced Renal Damage and Nephrotoxicity—An Overview for Applied Toxicology. *AAPS J.* **2011**, *13*, 615–631. [[CrossRef](#)] [[PubMed](#)]
27. Delgado, C.A.; Balbuena Guerreiro, G.B.; Diaz Jacques, C.E.; de Moura Coelho, D.; Sitta, A.; Manfredini, V.; Wajner, M.; Vargas, C.R. Prevention by L-carnitine of DNA damage induced by 3-hydroxy-3-methylglutaric and 3-methylglutaric acids and experimental evidence of lipid and DNA damage in patients with 3-hydroxy-3-methylglutaric aciduria. *Arch. Biochem. Biophys.* **2019**, *668*, 16–22. [[CrossRef](#)] [[PubMed](#)]
28. Racusen, L.C.; Finn, W.F.; Whelton, A.; Solez, K. Mechanisms of lysine-induced acute renal failure in rats. *Kidney Int.* **1985**, *27*, 517–522. [[CrossRef](#)] [[PubMed](#)]
29. Grünert, S.C.; Schlatter, S.M.; Schmitt, R.N.; Gemperle-Britschgi, C.; Mrázová, L.; Balci, M.C.; Bischof, F.; Çoker, M.; Das, A.M.; Demirkol, M.; et al. 3-Hydroxy-3-methylglutaryl-coenzyme A lyase deficiency: Clinical presentation and outcome in a series of 37 patients. *Mol. Genet. Metab.* **2017**, *121*, 206–215. [[CrossRef](#)]
30. Da Rosa, M.S.; Seminotti, B.; Amaral, U.; Fernandes, C.G.; Gasparotto, J.; Moreira, C.F.; Gelain, D.P.; Wajner, M.; Leipnitz, G. Redox homeostasis is compromised in vivo by the metabolites accumulating in 3-hydroxy-3-methylglutaryl-CoA lyase deficiency in rat cerebral cortex and liver. *Free. Radic. Res.* **2013**, *47*, 1066–1075. [[CrossRef](#)] [[PubMed](#)]

**Disclaimer/Publisher's Note:** The statements, opinions and data contained in all publications are solely those of the individual author(s) and contributor(s) and not of MDPI and/or the editor(s). MDPI and/or the editor(s) disclaim responsibility for any injury to people or property resulting from any ideas, methods, instructions or products referred to in the content.